Hyperfine fields at transition-element impurities in Gd†

W. D. Brewer and E. Wehmeier
Fachbereich Physik der Freien Universität Berlin, Berlin, West Germany
(Received 23 April 1975)

Low-temperature nuclear-orientation measurements on a number of dilute alloys of $3d$ and $4d$ transition elements in Gd host are reported. The derived hyperfine fields in kG are: *Gd*V, -87.4 ± 9.2; *Gd*Cr, $+23.1\pm5.4$.; *Gd*Mn, $+186.4\pm4.3$; *Gd*Y, -150 ± 7; *Gd*Zr, -100 ± 15; *Gd*Nb, -92.9 ± 0.8; *Gd*Mo, $+49\pm6$ or -40 (see text); and *Gd*Tc, $+87.6\pm2.9$. In addition, a Mössbauer-effect source experiment gives for *Gd*Fe a hyperfine field of 0 ± 16 kG. These results nearly complete the systematics for $3d$ and $4d$ impurities in Gd host, and support the model for Gd proposed by Campbell. We discuss the derived values of local moments for $3d$ and $4d$ impurities in Gd.

I. INTRODUCTION

Since the development about 1960 of widely applicable methods for determining hyperfine fields at impurity nuclei in ferromagnetic metal hosts, the systematic variations of the fields with impurity Z in the host metals Fe and Ni have been well established.[1] These systematics have been explained qualitatively as arising from the combination of conduction-electron polarization (CEP) and core polarization (CP) fields.[2,3] In contrast, measurements of hyperfine fields in Gd host have been relatively few in number, primarily due to the difficult metallurgy and the low solubilities of most elements in Gd, which rules out NMR and Mössbauer-absorber experiments in most cases. Several fields in Gd have recently been measured using perturbed angular correlations[4] (PAC) and implantation perturbed angular correlations[1,5] (IMPAC), as well as a few by nuclear orientation[6-8] and Mössbauer-source experiments.[1]

Campbell[9] has proposed a model for the systematics of fields at s-p impurities in Gd, and more recently, for the hyperfine fields at d-transition impurities in this host,[7,10] the latter based on positive f-d interactions and d-d coupling between the Gd moments, leading to the expectation that the hyperfine field vs impurity Z curve in Gd should resemble that for Fe or Ni hosts, but with the sign of the local moment (CP) contribution reversed. In a recent paper,[7] this model was shown to agree with existing data for $3d$ and $5d$ impurity fields; however, the available data were unfortunately rather incomplete.

We report here new measurements of the hyperfine fields at nuclei of the $3d$ transition elements V, Cr, and Fe in Gd host, and a remeasurement of the field for *Gd*Mn which verifies the sign and magnitude reported earlier.[7,8] With these results, the systematics for *Gd*($3d$) hyperfine fields are complete except for the difficult cases Ti and Ni, and for Cu, which can in any case be estimated with some confidence from the known fields on Ag and Au in Gd and Fe and on Cu in Fe. The determinations were made by the nuclear-orientation method except for *Gd*Fe, which was determined in a Mössbauer-source experiment.

In the $4d$ series, we have determined hyperfine fields at nuclei of Y, Zr, Nb, Mo, and Tc impurities in Gd using nuclear orientation. The *Gd*Nb result is nearly a factor of 2 larger than a previously determined value,[8] and is supported by measurements over a large range of temperatures and applied fields. The *Gd*Mo result also differs from that obtained by perturbed angular correlations,[4] but may be analyzed as resulting from two distinct sites for the Mo impurities. These measurements, together with other work,[4,8] complete the systematics for second-transition-series impurities in Gd host.

By making the assumption that the dominant contributions to the hyperfine fields are those of the host (CEP) and the local moment (CP), one can derive values for the local moments formed by transition-element impurities. This procedure and the results for $3d$ and $4d$ impurities are discussed in the final section of the paper.

II. EXPERIMENTAL

Two sources for most of the nuclear-orientation experiments were prepared, starting with 99.9% Gd and carrier-free solutions of the radioisotopes (except ^{51}Cr and ^{89}Zr). Ingots of Gd were activated by electroplating or adding pieces of irradiated target material, or by drying on activity from a methanolic solution. They were then melted by induction heating on a water-cooled copper hearth in high-purity Ar atmosphere. After repeated melting and rapid cooling, the alloys were flattened to disks 1 mm thick, which were tinned on both sides with In using an ultrasonic soldering gun. A nuclear thermometer alloy (*Fe*^{60}Co or *Ni*^{54}Mn) was soldered to one face and the other was attached to a silver sample holder and mounted in adiabatic demagnetization cryostat. The samples were

TABLE I. Sample preparation and data analysis.

Sample	Activation method	Impurity conc. (at. ppm)	Nuclear parameters			
			I	μ_I (μ_N)	$t_{1/2}$	U_2F_2, U_4F_4
Gd^{48}V I	electroplated	0.62	4	1.63	16.2 day	−0.3752, −0.1451
Gd^{48}V II	evaporated	0.39				
Gd^{51}Cr I	active Cr metal	80.1	7/2	0.933	27.7 day	+0.5567, +0.0093
Gd^{51}Cr II	evaporated	0.04				
Gd^{54}Mn I	electroplated	0.25	3	3.302	303 day	−0.4925, −0.4398
Gd^{54}Mn II	evaporated	0.06				
Gd^{57}Co I	evaporated	15.0				
Gd^{57}Co II	evaporated	5.0				
Gd^{88}Y	evaporated	10^{-2}	4	0.89 ± 0.14	108 day	−0.4477, −0.0304
Gd^{89}Zr (+$^{89}Y^m$)	active Y metal	6200 (Y)	9/2 (9/2)	1.06 ± 0.15 (6.2 ± 0.5)	3.27 day (16 sec)	−0.9358, +0.5322
Gd^{95}Zr	evaporated	0.02	5/2	1.3 ± 0.2	64 day	$+0.2376^{+0.1139}_{-0.1169}$
Gd^{95}Nb	electroplated	0.01	9/2	6.3 ± 0.1	35 day	+0.226
$Gd^{93}Mo^m$	electroplated	10^{-5} (< 5 Nb)	21/2	9.21 ± 0.2	6.9 h	−0.7924, (γ_1) +0.2984
Gd^{96}Tc	electroplated	10^{-4} (< 10 Nb)	7	5.37 ± 0.17	4.3 day	−0.3905, −0.1874

cooled to 7–12 mK in applied fields of 15–60 kOe and maintained below 20 mK for up to 16 h. Normalization counts at 4.2 K were taken for several hours before and after each demagnetization. The data were analyzed on the assumption of a purely magnetic hyperfine interaction with a single hyperfine field at all impurity sites. Details of sample preparation and the nuclear parameters used in the data analysis are shown in Table I.

For the Mössbauer experiments, two sources of Gd^{57}Co were made, starting with 99.9%-Gd foil and repurified carrier-free ^{57}Co solutions. The activity was evaporated from methanolic solution onto a small piece of Gd foil, which was then wrapped in a larger piece of foil and melted several times in an argon arc furnace equipped with a thoriated W electrode and a water-cooled Cu baseplate. The ingots were flattened and rolled to a thickness of 50 μm. One alloy (sample II) was used in this form, while the other was annealed for 3 h at 900 °C in Ar atmosphere and then further rolled to 25 μm thickness. Each source was soldered onto a Cu backing plate with In, and mounted in a cryostat with a Be window. Mössbauer spectra were taken with the sources at 296 and 77 K in zero applied field against an ^{57}Fe-enriched stainless-steel absorber at room temperature.

III. DATA ANALYSIS AND RESULTS

The data obtained from the nuclear-orientation experiments consist of normalized γ-ray counting rates at a particular angle relative to the applied field H_0, as a function of H_0 and sample temperature. For a given (unique) hyperfine field and a magnetically saturated sample, the counting rates (anisotropies) are given by the usual formula

$$W(\theta) = 1 + \sum_{k=2}^{k_m} B_k (H_{eff}/T)\, U_k F_k\, P_k(\cos\theta), \qquad (1)$$

where $U_k F_k$ are constants depending on the decay scheme of the radioactive nucleus (Table I), P_k are Legendre polynomials, and B_k are orientation tensors, which are known functions of the nuclear moment and the ratio of the total field H_{eff} at the nucleus to the sample temperature. The maximum value of the index k depends on the decay scheme and is usually $k_m = 4$; due to parity conservation, only even values of k occur for γ radiation. The field H_{eff} is given by

$$H_{eff} = \left| |H_{hf}| \pm (H_0 - D_m) \right| , \qquad (2)$$

where the + sign indicates a positive hyperfine field. The demagnetizing field D_m was about 1.2 kG for our samples and the reported values of

H_{hf} are corrected accordingly.

In the event that more than one value of H_{hf} exists at different impurity sites, or that $\vec{H}_{hf}$ is not parallel to $\vec{H}_0$ at all sites (unsaturated local magnetization), or if a significant electric quadrupole interaction is present, formula (1) must be modified by suitable averaging of B_k and P_k or by modifying the form of B_k. For example, for a sample with two distinct lattice sites a and b and corresponding effective fields H_a, H_b, with fraction α of the impurity nuclei in site a, the measured anisotropy is given by

$$\bar{W}(\theta) = 1 + \sum_k U_k F_k P_k(\cos\theta) \times [\alpha B_k(H_a/T) + (1-\alpha) B_k(H_b/T)]. \quad (3)$$

If $\bar{W}$ is then analyzed in terms of a single apparent hyperfine field $\bar{H}_{hf}$, the latter will show a dependence on H_0 and T which will depend on the decay scheme of the isotope observed. A similar conclusion holds for incomplete saturation of the local magnetization, or for mixed magnetic-dipole–electric-quadrupole interactions. Thus the appearance of a temperature or field dependence in the derived H_{hf} values, or of a dependence on decay scheme if several different radiations are observed, or, of course, a dependence on impurity concentration, may be taken as an indication that the H_{hf} value is not representative of the correct magnetic hyperfine field for the impurity in substitutional sites. Such tests are very important in evaluating nuclear-orientation data, since the method measures an integral quantity over the entire sample, and may otherwise yield misleading or false results.

The results of the experiments on each transition impurity will be treated separately below, since they represent a variety of distinct problems in data analysis.

A. *Gd* V

For this case two samples of various concentration were prepared using commercially available ^{48}V activity (16-day half-life). The decay scheme and nuclear moment are well known. Both samples gave temperature-independent consistent results although the relatively large statistical errors did not permit an unambiguous determination of the sign of H_{hf}. From systematics, the − sign appears to be much more likely. The derived values are shown in Table II.

B. *Gd*Cr

Two samples were prepared, in one case using irradiated natural Cr metal, in the other using a commercial ^{51}Cr solution (28 day). The results were again consistent and temperature independent and indicated a positive hyperfine field (Table II).

C. *Gd* Mn

This system was studied previously by Stone and Marsden[7,8] who found a value $H_{hf} = +186 \pm 4$ kG. In view of the relatively narrow range of applied fields used in their measurements (10–20 kOe) and the concomitant danger of unsaturated local magnetization, as well as the possibility of compound formation in this alloy, a redetermination was felt to be of value. The first sample, made using commercial 303-day ^{54}Mn, gave a temperature-dependent hyperfine field. A plot of H_{eff} vs H_0 also did not show the slope expected from Eq. (2) (see Fig. 1). A second sample of much lower Mn concentration gave temperature-independent results with the correct slope as a function of applied field, leading to a value of H_{hf} in excellent agreement with the previously reported result. Both samples unambiguously confirmed the + sign reported in Ref. 7.

D. *Gd* Fe

No suitable iron isotope for nuclear orientation exists, so a Mössbauer-effect-source experiment was performed. The two *Gd* ^{57}Co sources gave essentially identical Mössbauer spectra; typical examples are shown in Fig. 2, together with a *Ni*Fe ($H_{hf} = 283$ kG) calibration spectrum. The *Gd*Fe spectra are unresolved but show considerable broadening even above the Curie temperature ($T = 294$ K). This is probably due to a combination of quadrupolar splitting and fluctuations from the ferromagnetic transition near T_c. At 77 K the line is only slightly broader, indicating that the hyperfine field is small. While a sign determination in applied field might be possible, it would be complicated by the relatively large saturation field of polycrystalline Gd and thus was not attempted. Attributing the line broadening between 296 and 77 K to the magnetic hyperfine interaction, we obtain $|H_{hf}| \leq 16$ kG or $H_{hf} = 0 \pm 16$ kG. If the remaining excess linewidth at 296 K is due to quadrupolar broadening, the electric field gradient (EFG) $|eq_0|$ at Fe in Gd would be about 0.7×10^{17} V/cm^2, using $\gamma_\infty = -5.2$ for Fe and $Q(\frac{3}{2}) = 0.2$ b. This value is somewhat smaller than calculated for the point charge model for Gd, but agrees well with the measured EFG in the metal,[11] which gives confidence in the source preparation and spectrum analysis.

E. *Gd* Y

For this determination, commercial 108-day ^{88}Y was used. Sample preparation difficulties are minimal, since Y is completely miscible with Gd.[12] The decay scheme of ^{88}Y is well known, and the magnetic moment of the 4 − state was calculated to be $\mu_{(4-)} = (0.89 \pm 14)\ \mu_N$ using known single-particle moments of ^{87}Sr ($N = 49$, $\mu_{(9/2)} = -1.093$) and ^{89}Y ($Z = 39$, $\mu_{(1/2)} = -0.138$). The effective

TABLE II. Impurity hyperfine fields and derived moments for $Gd(3d)$ and $Gd(4d)$ alloys.

Impurity	H_{hf} (kG)	H_{cp} (kG)	R_{cp} (kG/μ_B)	μ (μ_B)
Sc	-60.2 ± 4.0[a]	-16 ± 5	-55 ± 20	$+0.29^{+0.31}_{-0.14}$
Ti	-90 ± 10[b]	-37 ± 10	-60 ± 20	$+0.62^{+0.56}_{-0.28}$
V	-87.4 ± 9.2[c] $(+21.7\pm7.9)$	-32 ± 9	-65 ± 20	$+0.49^{+0.35}_{-0.17}$
Cr	$+23.1\pm5.4$[c]	$+86\pm6$	-70^{+20}_{-30}	$-1.23^{+0.42}_{-0.49}$
Mn	$+186.4\pm4.3$[a,c]	$+254\pm5$	-75^{+25}_{-30}	$-3.39^{+1.02}_{-2.79}$
Fe	0 ± 16[c]	$+74\pm20$	-80^{+25}_{-30}	$-0.93^{+0.44}_{-0.78}$
Co	-42.5 ± 4.0[a]	$+38\pm5$	-85^{+30}_{-25}	$-0.45^{+0.15}_{-0.33}$
Ni	-72 ± 5[b]	$+15^{+4}_{-6}$	-85 ± 30	$-0.18^{+0.09}_{-0.28}$
Cu	-90 ± 5[d]	...	-90 ± 30	0
Y	-150 ± 7[c]	$+7\pm7$	-370 ± 40	0 ± 0.04
^{89}Zr	-104 ± 27[e]	$+62\pm20$	-370 ± 40	$-0.17^{+0.07}_{-0.08}$
^{95}Zr	-99 ± 15[c]			
Nb	-92.9 ± 0.8[c]	$+71\pm5$	-370 ± 40	$-0.19^{+0.03}_{-0.04}$
Mo	-40[f] $(+49.2\pm5.9)$[c]	$+126\pm10$	-370 ± 40	$-0.34^{+0.06}_{-0.07}$
Tc	$+87.6\pm2.9$[c]	$+264\pm5$	-370 ± 40	$-0.71^{+0.08}_{-0.11}$
Ru	$+50\pm10$[g] $+270\pm90$[h]	$+232-1450$	-370 ± 40	$-0.57--1.36$
Rh	$+61\pm5$[g]	$+250\pm10$	-370 ± 40	$-0.68^{+0.09}_{-0.11}$
Pd	-66 ± 8[g]	$+128\pm10$	-370 ± 40	$-0.35^{+0.06}_{-0.07}$
Ag	-198 ± 8[i]	...	-370 ± 40	0

[a]From Ref. 7.
[b]Estimated from systematics curve, Fig. 4.
[c]From present work (errors quoted are rms deviations from mean values and are comparable with statistical errors).
[d]Estimated from $4d$, $5d$ fields (Ref. 7).
[e]Assuming no reorientation in $16s$ metastable state.
[f]Derived using two-sites model (see text).
[g]PAC determination, Ref. 4.
[h]IMPAC determination, Ref. 5.
[i]From Ref. 8.

field data showed considerable scatter, in particular at low applied fields, so only the high-field data were used to obtain the result shown in Table II. The total error in H_{hf} [including the uncertainty in the estimate of $\mu(4+)$] is about ± 24 kG.

F. *Gd* Zr-*Gd* Y

The decay of 3-day ^{89}Zr offers the possibility of determining the hyperfine field at either Zr or Y, depending on the nuclear-spin–lattice relaxation time T_1 of *Gd*Y. The decay passes through the 16-sec metastable state $^{89}Y^m$, which will show some reorientation if $T_1 \leq 500$ sec and essentially complete reorientation for $T_1 \leq 15$ sec. The nuclear moments of the two states were estimated from the single-particle model to be ^{89}Zr, $\mu_{(9/2)} = (1.06 \pm .15)\mu_N$, $^{89}Y^m$, $\mu_{(9/2)} = (6.2\pm0.5)\mu_N$. The activity was prepared by a $(d, 2n)$ reaction on natural Y foil using 15-MeV deuterons at the Karlsruhe Cyclotron, and a piece of the target foil was melted directly into the sample. The resulting anisotropy was completely attributable to the ^{89}Zr parent state (the anisotropy curves for the two states differ considerably) and yielded the value shown in Table II for H_{hf}, as well as the result that T_1 is long (several hundred seconds at 15 mK).

G. *Gd* Zr

The solubility of Zr in Gd is of order 1%,[12] so in this system the alloy preparation is uncompli-

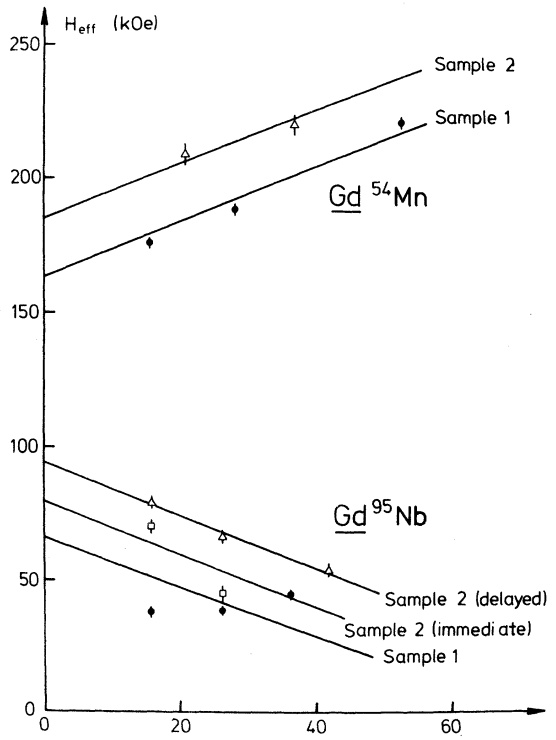

FIG. 1. Effective (net) field data for several alloys showing the dependence on applied field [Eq. (2)]. Upper portion: *Gd*Mn, two samples. Sample 1 showed temperature dependence and has the wrong slope of H_{eff} vs H_0. The zero-field intercept of the straight line fit gives $|H_{hf}|$. Lower portion: three sets of experiments on *Gd*Nb. Only the third set (uppermost curve) showed no temperature dependence and the correct slope of H_{eff} vs H_0. Here H_{hf} is negative.

cated. A commercial solution of 64-day ^{95}Zr was used for activation of the sample. The nuclear moment of ^{95}Zr was estimated from the analog state in ^{91}Zr to be $\mu_{(5/2)} = (-1.3 \pm 0.2)\mu_N$. The $M1$-$E2$ admixtures of the 724- and 757- keV γ rays have been determined[13] and were used to calculate the anisotropy coefficients (Table I); this introduces some uncertainty into the data analysis. The sign of the field could not be unambiguously determined but is almost certainly negative. The value thus derived agrees well with that determined for ^{89}Zr (Table II, the error shown is statistical only).

H. *Gd*Nb

The 35-day isotope ^{95}Nb is very suitable for nuclear orientation and may be obtained either in pure form or as the daughter activity from the decay of ^{95}Zr. A previous experiment using ^{95}Nb activity (Ref. 8) gave $H_{hf} = -51 \pm 5$ kG for $10 \leq H_0 \leq 20$ kOe. Our first sample, prepared as in Ref. 8, gave a similar value at 15 kOe applied field but showed a temperature-dependent hyperfine field and the wrong slope in a plot of H_{eff} vs H_0 (Fig. 1). A second sample was made using a mixture of ^{95}Nb-Zr activities, which showed systematically larger effective fields than the first alloy, but still gave the wrong slope as a function of H_0. This sample was then stored for several months to allow the original ^{95}Nb to decay, so that the only ^{95}Nb activity present was due to the decay of ^{95}Zr. The much higher solubility of Zr in Gd and the lack of compound formation give reason to expect better results from a sample in which Zr was alloyed with Gd. The fields obtained were in fact temperature independent and gave a good fit to Eq. (2) (see Fig. 1), leading to a value of H_{hf} about 80% higher than that earlier reported, but which is most probably near to the correct value in view of its temperature and field behavior.

I. *Gd*Mo

This system has been investigated by perturbed angular correlations[4] using ^{95}Mo fed from the decay of 61-day ^{95}Tc. The results were inconclusive, giving a positive hyperfine field of about 30 kG using tempered samples, and a small negative field (approximately -10 kG) with rapidly quenched samples. The authors[4] attributed this to compound formation with the Tc parent in the tempered samples, and concluded that the negative fields were more probably representative of dilute *Gd*Mo. An IMPAC measurement has also been reported[5]; it

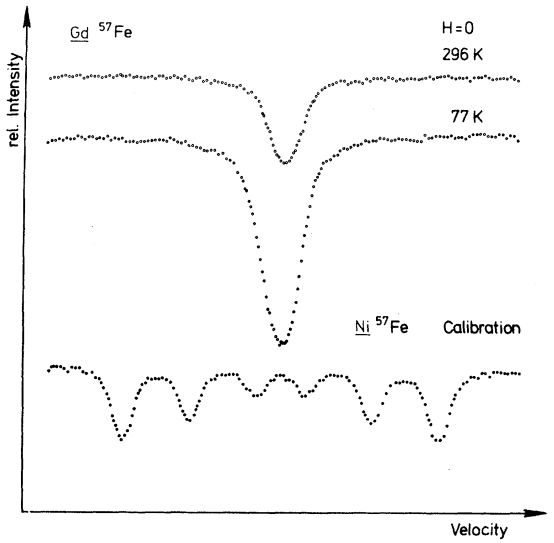

FIG. 2. Zero-field Mössbauer spectra of *Gd* ^{57}Co sources vs ^{57}Fe (stainless-steel) absorber, for two source temperatures. The absorber was at room temperature. Lower curve: calibration spectrum from a *Ni* ^{57}Co source.

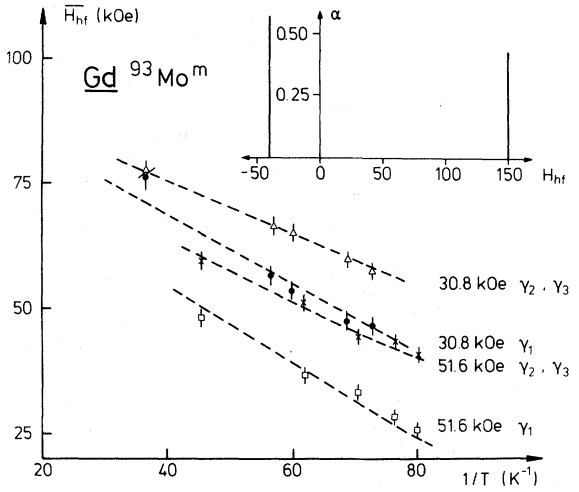

FIG. 3. Data for apparent hyperfine field $\overline{H}_{hf}$ in *Gd*Mo, plotted against $1/T$ to show temperature dependence, for several values of H_0 and different γ rays. The lines are calculated values assuming two impurity sites with distinct hyperfine fields. Inset: hyperfine field distribution for which the best fit to the data were obtained: site *a*, $H_{hf} = +150$ kG (43%); site *b*, $H_{hf} = -40$ kG (57% occupation).

indicated a large negative field.

We have used the 7-h isotope ^{93}Mo^{m}, which has an extremely favorable decay scheme for nuclear orientation and for which the parameters are well known.[14] The isotope was obtained with high specific activity from the $(d, 2n)$ reaction on natural Nb foils using 11-MeV deuterons at the Cyclotron Laboratory of the Technische Universität Berlin, and was separated from the target material by ion exchange chromatography. It was hoped that the extremely low Mo concentration and rapid quenching of the alloys would yield a reliable value for H_{hf}, but this proved not to be the case: The hyperfine fields obtained were strongly dependent on temperature, applied field, and on the γ-ray transition observed. (The 263-keV γ_1 has different anisotropy coefficients from the 685- and 1477-keV γ_2 and γ_3 transitions.) The data points as a function of inverse temperature for the various γ transitions and two applied fields are shown in Fig. 3, along with a fit using the model given by Eq. (3), with $H_a = \pm 150$ kG, $H_b = -40$ kG, and $\alpha = 43\%$ (see inset, Fig. 3). This model is able to fit the observed temperature-, field-, and decay-scheme dependence extremely well, giving an rms deviation per point of 0.5 kG. Of course the model is not unique, and other hyperfine field distributions would undoubtedly give equally good fits to the data. (Other hypotheses, such as incomplete local magnetization or an additional quadrupole interaction, can be ruled out on the basis of the form of the observed dependence on T and H_0.) The hypothesis of two distinct hyperfine fields is the simplest explanation of the data, however, and is physically reasonable in view of results on implanted impurities, for example. While the exact value of H_{hf} must be regarded as still undetermined, we regard $H_{hf} = -40$ kG as being in all probability near to the correct value for dilute *Gd*Mo. The other site, with $H_{hf} \simeq +150$ kG, is no doubt a nonsubstitutional impurity location, or, more probably, an intermetallic compound. The value $\overline{H}_{hf}$ obtained by a straightforward data analysis using Eq. (1) is also shown in Table II.

J. *Gd*Tc

For this alloy, the 4-day isotope ^{96}Tc was used. The decay parameters and nuclear moment are well known.[15] The activity was prepared by the (α, n) reaction on Nb foil using 19-MeV α at the Karlsruhe Cyclotron, followed by separation with ion exchange. The hyperfine fields derived showed no temperature or field dependence and indicated an unambigous + sign.

IV. DISCUSSION

The hyperfine fields obtained in this work are summarized in Figs. 4 and 5 and in Table II, along with those reported in Ref. 4 (Ru, Rh, Pd), Ref. 7 (Sc, Mn, Co), and Ref. 8 (Ag), and estimates from systematics for the Ti, Ni, and Cu fields. The dashed line in Fig. 4 is simply a smooth curve drawn through the data points and is essentially identical to the systematics curve given in Fig. 1, Ref. 7. The solid line represents the estimated CEP contribution to H_{hf}. The new values agree remarkably well with those predicted in Ref. 7 on

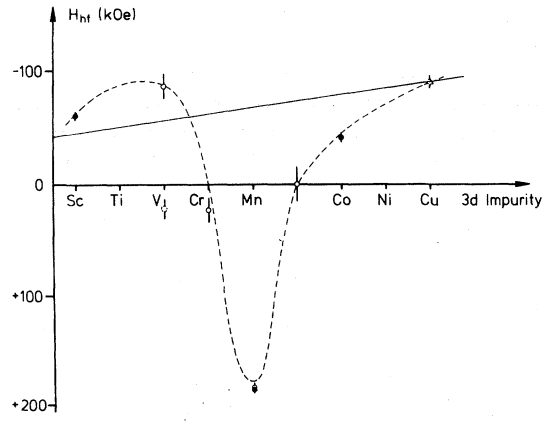

FIG. 4. Systematics of impurity hyperfine fields in Gd host for 3*d* series impurities. Solid circles are from Ref. 7, open circles from present work. The value for *Gd*Cu was estimated in Ref. 7 by comparison with *Gd*Au, *Gd*Ag, and *Fe*Cu fields. The dotted point for *Gd*V is the value that would result if the field were assumed positive.

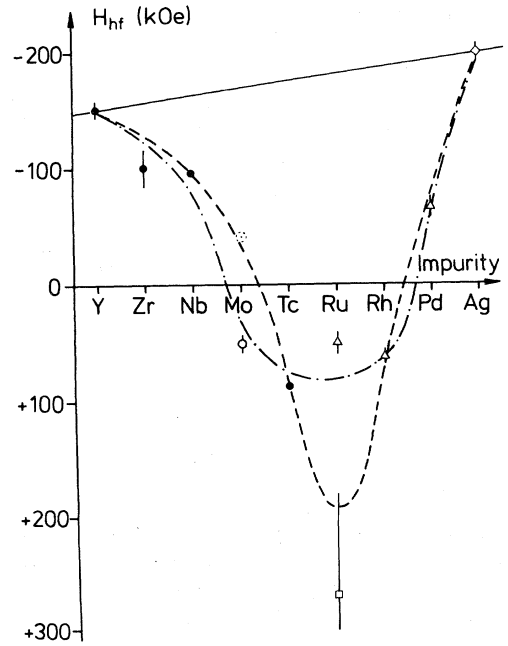

FIG. 5. Systematics plot for 4*d* series. Solid circles from present work, open circle (Mo): apparent value $\bar{H}_{hf}$, dotted circle from two site model (see text and Fig. 3). Triangles: from Ref. 4; square: IMPAC measurement (Ref. 5); *Gd*Ag from Ref. 8.

the basis of the then-available data.

Figure 5 shows the fields for the 4*d* series. The two dashed lines are again attempts to draw a smooth curve through all the points. This is not nearly as successful as in the 3*d* series, primarily because of the uncertainty in the Mo field and the fact that neither of the two reported values for *Gd*Ru seems to fit the systematics. Taking the *Gd*Mo field to be negative, as seems most probably correct, one is led to the sharply peaked dashed curve which closely resembles the corresponding curve for 4*d* impurities in Ni; this would tend to favor the IMPAC value for *Gd*Ru. Taking the value for *Gd*Mo obtained from a straightforward analysis of our data, and placing more weight on the PAC result for *Gd*Ru, one obtains the broad, flat dot-dashed curve. The solid line, representing the CEP contributions to the fields, was drawn using an estimated field for *Gd*Sr of about −140 kG interpolated from *Gd*Ca and *Gd*Lu.

The local moments of 3*d* impurities in Gd can be estimated by taking the difference between the dashed and solid curves in Figs. 4 and 5; this difference gives that part of the hyperfine field which is due to local magnetism, essentially the core-polarization field H_{cp}. The main difficulty with the estimation of the moments themselves is the inaccuracy of the effective hyperfine field constants $R_{cp} = H_{cp}/\mu$, due to the uncertain effects of *s*-*d* mixing in the metallic environment. Neglect of the latter effect leads to underestimation of the local moment. Two other contributions to the net hyperfine field are the orbital field, due to spin-orbit coupling which reduces quenching of the *d*-shell orbital moments, and the spin-dipolar field which is not necessarily zero in hexagonal symmetry. Both of these contributions give positive hyperfine fields, and their neglect would tend to exaggerate the estimates of negative local moments and reduce the estimates of positive moments. The orbital contribution should be greater in the 4*d* series due to the larger spin-orbit coupling, while the spin-dipolar contribution may be smaller because of the greater spatial extension of the 4*d* wave functions. Keeping these limitations in mind, we can use the curves of Figs. 4 and 5 to estimate local moments.

The estimated core-polarization fields, R_{cp} values, and derived moments are also given in Table II. The errors in the moments include experimental errors in H_{hf} and the assumed uncertainties in R_{cp}. Neutron-diffraction measurements for Gd host are not available, because of the large nuclear neutron cross section in natural Gd and the low impurity solubilities; the present experiments thus represent the only moment data. The moment systematics are shown in Figs. 6 and 7 along with data for 3*d* and 4*d* impurities in Ni host.[3,16] As expected, the trend in Gd is roughly a mirror image of that in Ni. Several points deserve comment: the anomalously large magnitude of the Mn moment in Gd, the apparent shift of the *Gd*(3*d*) curve to lower impurity *Z* with respect to the Ni curve, and the relatively large and uniformly negative moments observed for the 4*d* elements in Gd.

Models for the interactions of impurity moments with the host conduction band in *d*-band host metals, based on the Clogston-Wolff theory, have been given by Moriya[17] and by Campbell and Gomes.[18] These models predict the general features of the curves shown in Fig. 6: vanishing moments at the ends of the series, increasing towards the middle, with a sign change near Mn. The predictions agree reasonably well with the data for 3*d* moments in Fe, Ni, and Pd hosts. Taking Gd as a *d* transition metal, one would expect similar results to apply, with the relative signs of host and impurity moments reversed, since Gd is at the beginning of a *d* series, in contrast of Fe, Ni, and Pd.

The sign and magnitude of the Mn moment is particularly sensitive to the assumed splitting and positions of the host subbands in these models; e.g., the predicted Mn moment is zero in Fe, about $-1.5\mu_B$ in Co, and nearly $+4\mu_B$ in Ni host.[18] Thus the moment observed for Mn in Gd is not necessar-

ily outside the framework of such a model.

The "crossover point" for 3*d* moments in Gd, observed between V and Cr in this work, is a more serious departure from the curves for 3*d* hosts. One possibility is that the different band structure of Gd leads to a rather smaller critical value of the excess impurity charge for "crossover," so that the observed curve would in fact be obtained from the above model if the calculation were carried out for Gd host. Of course, the model may also be inapplicable to Gd host in its present form; e.g., the exchange integrals J_{imp} and J_{host} were taken to be equal in Ref. 18, which is almost certainly a poor approximation for 3*d* impurities in Gd.

Another, in our opinion unlikely, possibility is that the sign of the Cr hyperfine field in Gd is actually negative; this assumption gives a much poorer fit to the data than a positive field, yielding $H_{\text{hf}} = -79 \pm 15$ kG. This in turn gives a Cr moment near zero and a moment curve for Gd host which is a nearly perfect mirror image of the curve for Ni host, as might be expected from the relative positions of Gd and Ni in their respective *d* series. Moment calculations for Gd should clear up this point.

In the 4*d* series, the question of the existence of localized moments remains unresolved. The values shown for Gd host in Fig. 7 are relatively uncertain, on the one hand because the orbital and spin dipolar contributions to the hyperfine field, mentioned above, tend to exaggerate the estimated moments, which are all negative; on the other hand, a constant and possibly inaccurate value of R_{cp} was used for the whole series.[3] Moments on Ru, Rh, and Pd have been observed in Fe host by neutron diffraction,[16] but their existence in Ni host is unclear and the Ni values in Fig. 7 were estimated from hyperfine fields. It seems likely that the estimated moments in Gd host shown in Fig. 7 are much too large, particularly for Zr, Nb, and Mo. Since Tc is in the middle of the series it represents an unstable situation analogous to Mn and no conclusion can be drawn. In any case, the tendency for the local contributions to the hyperfine field in Gd to be a mirror image of those in Ni host clearly continues in the 4*d* series.

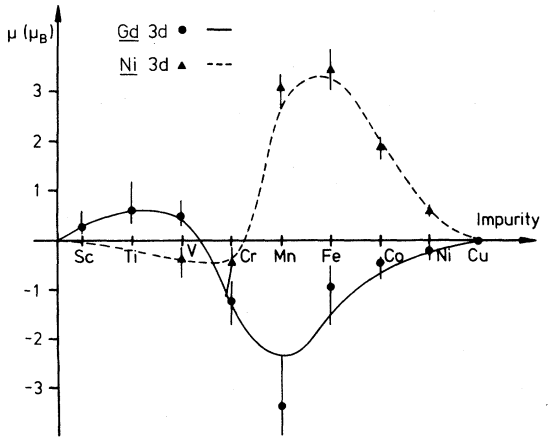

FIG. 6. Impurity moments on 3*d* transition impurities in Ni (triangles) and in Gd (circles). Gd values, this work and Ref. 7 (see Table II); Ni values from Refs. 3 and 16.

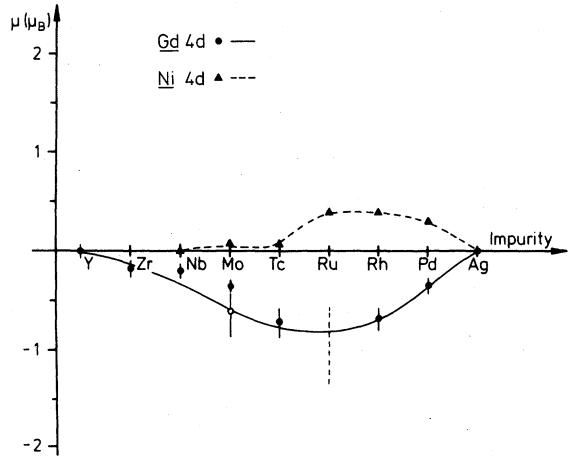

FIG. 7. Impurity moments on 4*d* transition impurities in Ni (triangles) and in Gd (circles). Gd values, this work and Refs. 4 and 8 (see Table II); Ni values from Refs. 1 and 3. The open circle for Mo is obtained using the apparent hyperfine field, the solid circle using the value from the two-sites model.

Our results thus strongly support the suggestion of Refs. 7 and 10, that the magnetic coupling in Gd is predominately through a *d*-*f* interaction and *d*-*d* coupling, and that Gd (seen from a substitutional impurity site) resembles a *d* transition metal at the beginning of the series.

This conclusion was given theoretical support by the recent work of Harmon and Freeman,[19] who have calculated the band structure and CEP of ferromagnetic Gd, as well as the *s*-*f* and *d*-*f* exchange integrals. They find that the *d*-*f* exchange is considerably stronger, and most of the CEP is borne by the *d*-like conduction electrons, in agreement with our conclusions based on experiment.

ACKNOWLEDGMENTS

Our interest in this work was stimulated by discussions with Dr. I. A. Campbell, whose suggestions we gratefully acknowledge. We thank G. Koopman for allowing the use of sample preparation facilities, and Professor E. Matthias for support of our group. We also acknowledge the assistance of the Cyclotron Laboratory, Gesellschaft für Kernforschung mbH, Karlsruhe, and of Prof-

fessor J. Ney, Dr. K.-D. Lennartz, and H. Norbert of the Cyclotron Group, Institut für Strahlungs- und Kernphysik, Technische Universität Berlin, in producing isotopes used in this work. Our Cr sample was irradiated at the FR-2 reactor in Karlsruhe.

---

†This work was supported in part by Der Bundesminister für Bildung und Wissenschaft.

[1]D. A. Shirley and T. Koster, tabulation of hyperfine fields in *Hyperfine Interactions in Excited Nuclei*, edited by G. Goldring and R. Kalish (Gordon and Breach, New York, 1971).

[2]D. A. Shirley and G. A. Westenbarger, Phys. Rev. 138, A170 (1965).

[3]D. A. Shirley, S. S. Rosenblum, and E. Matthias, Phys. Rev. 170, 363 (1968).

[4]L. Boström, K. Johansson, E. Karlsson, and L.-O. Norlin, in Ref. 1, p. 466; E. Karlsson *et al.*, contribution to the International Conference on Hyperfine Interactions, Uppsala, 1974 (unpublished); see also the review article by E. Karlsson, in *Proceedings of the Winter School on Nuclear Interactions with Extranuclear Fields, Zakopane*, 1973 (Polish Scientific Publishers, Warsaw, 1974), Chap. 8.

[5]G. M. Heestand, P. Hvelplund, B. Skaali, and B. Herskind, Phys. Rev. B 2, 3698 (1970).

[6]B. W. Marsden and N. J. Stone, Phys. Lett. A 35, 35 (1971).

[7]I. A. Campbell, W. D. Brewer, J. Flouquet, A. Benoit, B. W. Marsden, and N. J. Stone, Solid State Commun. 15, 711 (1974).

[8]B. W. Marsden, Ph. D. thesis (Oxford, 1971) (unpublished).

[9]I. A. Campbell, Phys. Lett. A 30, 517 (1969).

[10]I. A. Campbell, J. Phys. F 2, L47 (1972).

[11]J. Göring, Z. Phys. 251, 185 (1972).

[12]*Constitution of Binary Alloys*, edited by R. P. Elliot (McGraw-Hill, New York, 1965), Suppl. 1.

[13]W. Collin *et al.*, Ann. Phys. 15, 383 (1965).

[14]G. Kaindl, F. Bacon, and D. A. Shirley, Phys. Rev. C 8, 315 (1973).

[15]R. A. Fox, P. D. Johnston, D. J. Sanctuary, and N. J. Stone, in Ref. 1, Vol. 1, p. 341.

[16]G. G. Low and M. F. Collins, J. Appl. Phys. 34, 1195 (1963); I. A. Campbell, Proc. Phys. Soc. Lond. 89, 71 (1968).

[17]T. Moriya, Progr. Theor. Phys. 34, 329 (1965).

[18]I. A. Campbell and A. A. Gomès, Proc. Phys. Soc. Lond. 91, 319 (1967); I. A. Campbell, J. Phys. C 1, 687 (1968).

[19]B. N. Harmon and A. J. Freeman, Phys. Rev. B 10, 1979 (1974); Bull. Am. Phys. Soc. 19, 20 (1974).